Article

Threshold of Microvascular Occlusion: Injury Size Defines the Thrombosis Scenario

Aleksey V. Belyaev,[1,2,*] Mikhail A. Panteleev,[1,2,3,4] and Fazly I. Ataullakhanov[1,2,3,4]
[1]Center for Theoretical Problems of Physicochemical Pharmacology RAS, Moscow, Russia; [2]Federal Research and Clinical Center of Pediatric Hematology, Oncology and Immunology, Moscow, Russia; [3]Department of Physics, M. V. Lomonosov Moscow State University, Moscow, Russia; and [4]HemaCore LLC, Moscow, Russia

ABSTRACT Damage to the blood vessel triggers formation of a hemostatic plug, which is meant to prevent bleeding, yet the same phenomenon may result in a total blockade of a blood vessel by a thrombus, causing severe medical conditions. Here, we show that the physical interplay between platelet adhesion and hemodynamics in a microchannel manifests in a critical threshold behavior of a growing thrombus. Depending on the size of injury, two distinct dynamic pathways of thrombosis were found: the formation of a nonocclusive plug, if injury length does not exceed the critical value, and the total occlusion of the vessel by the thrombus otherwise. We develop a mathematical model that demonstrates that switching between these regimes occurs as a result of a saddle-node bifurcation. Our study reveals the mechanism of self-regulation of thrombosis in blood microvessels and explains experimentally observed distinctions between thrombi of different physical etiology. This also can be useful for the design of platelet-aggregation-inspired engineering solutions.

INTRODUCTION

Living systems at all levels of their organization display rich dynamic behavior, governed by various mechanisms of self-regulation, which are crucial for their functioning. An interesting example of such a phenomenon is hemostasis, which is aimed at prevention of bleeding via aggregation of blood platelets and fibrin network formation (1,2). However, under certain circumstances, an overgrown intravascular aggregate, called a thrombus, may cause dangerous conditions, for example, complete blockage of a blood vessel (vascular occlusion). Experimental data (3–8) on thrombosis are highly controversial, indicating the complexity and hierarchy of the involved physical and biochemical processes. It is not yet understood why some thrombi completely block the bloodstream, with possibly catastrophic consequences (3,4), and others accomplish their function without breaching the circulation (5–8). Several suppositions have emerged in an attempt to explain these observations. The mechanism of self-regulation of thrombosis has been ascribed to biochemical reactions and platelet activation (7,9), the changing porosity of the thrombus (10), or the nonuniform structure of the thrombus (6–12), but it is still a subject of debate. Early studies demonstrated that thrombosis is governed mainly by two competing factors: the rate of platelet attachment from the bloodstream and the intensity of hydrodynamic forces that prevent platelets from adhering to the thrombus (8,12–17). It was revealed that platelet aggregation rate does not simply increase with blood-flow velocity; rather, it exhibits a maximum with a subsequent decrease due to the growing hydrodynamic forces that inhibit platelet adhesion (13,14,18). The combination of hydrodynamic features of microvasculature and nonlinear shear-dependent platelet aggregation rate may, in principle, stop the growth of a thrombus. In this study, we use mathematical modeling to check the validity of this hypothesis and focus on principal physical effects that drive thrombosis.

MATERIALS AND METHODS

Blood flow

We account for closure of the blood circulatory system and deduce hydrodynamic conditions within the thrombotic vessel (Fig. 1 *a*). The heart acts as a pump, providing a systole-averaged constant flow rate, Q_0 (Fig. 1 *b*). We neglect pulsations in the microvasculature because of their small relative amplitude (8,19,20). A thrombotic vessel consists of a stenosed segment (with resistance R_x) and two healthy segments (R' and R''). A large number of healthy vessels with overall resistance $R_w \sim 100$ Pa·s/cm^3 (21) provide a shunt through which blood can bypass a thrombotic vessel. In our study, R_w is assumed constant in time, as we neglect the flexibility of vessel walls in microvasculature with respect to stenosis caused by the thrombus, so the radii of healthy vessels remain unchanged. The resistance of bigger vessels may be negligible compared to that of microvasculature. We restrict our analysis to arterioles and venules with diameters <1000 μm and >50 μm, for which Reynolds numbers are small (Re<0.1) (20), so flows are governed by quasistationary Stokes equations. For such vessels, we also have no option of entanglement of red blood cells in the fibrin network, which is typical for venous thrombi.

We approximate blood rheology in our model as Newtonian, i.e., characterized by a Navier-Stokes model. This should be treated as a simplifying assumption for initial study. However, we expect it to be a reasonable

Submitted April 21, 2015, and accepted for publication June 10, 2015.

*Correspondence: aleksey_belyaev@yahoo.com

Editor: Stanislav Shvartsman.

0006-3495/15/07/0450/7 $2.00

http://dx.doi.org/10.1016/j.bpj.2015.06.019

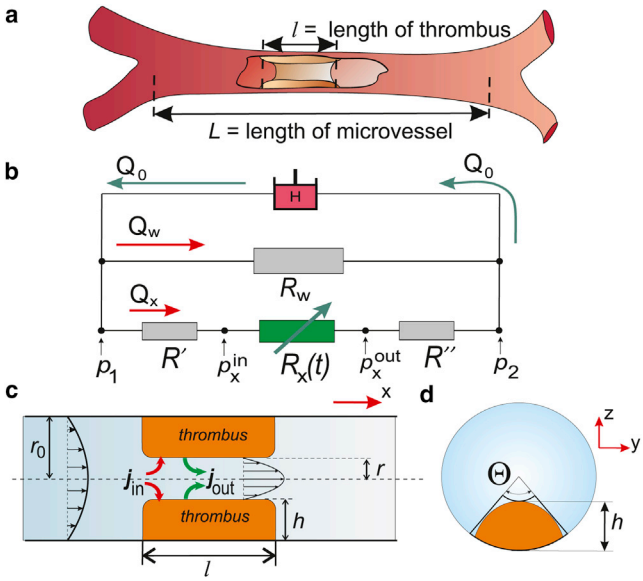

FIGURE 1 Scheme of the model. (*a*) Sketch of blood vessel with thrombus. (*b*) Hydraulic scheme of the circulatory system. The thrombotic vessel is depicted as a series of resistances, R', R_x, and R''; blood can bypass this resistance through the remaining healthy microvasculature, R_w. (*c*) Schematic side view of a thrombotic vessel with axisymmetric thrombus: $r(t)$ is the radial coordinate of the thrombus apex, h is the height of the thrombus, and r_0 is the radius of the vessel. (*d*) Schematic cross section of a thrombotic vessel: Θ is the angular size of the thrombus. The axisymmetric thrombus in (*c*) is a particular case, corresponding to $\Theta = 2\pi$. To see this figure in color, go online.

approximation for high shear rates (>100 s^{-1}), based on data from Fung (22).

Let L be the length of a thrombotic blood vessel measured between two consequent bifurcations. Healthy segments have a circular cross section, and the lumen shape of the stenosed segment is disturbed by the thrombus (Fig. 1 *c* and *d*). In our numerical model, the actual shape of the thrombus is approximated by a cylindrical segment protruding into the vessel and characterized by l, r, and Θ. The angular size of the thrombus, Θ, and its height, h, are allowed to change in time, whereas l remains constant. Resistance of the damaged segment, $R_x(t)$, changes due to growing stenosis, with consequent changes in pressure and flow rate in the whole circulatory system. The pressure difference between the vessel ends, $\Delta p_{12} = p_1 - p_2$, may change due to the thrombus, as well as the pressure drop across the thrombus, $\Delta p_x = p_x^{in} - p_x^{out}$, and the flow rate, Q_x, through the vessel (9). Thus, hydrodynamics and thrombus growth are coupled and should be considered within a unified self-consistent model. In our approach, at each time step for a given thrombus configuration, hydrodynamic values (shear rate, Δp_x, and Q_x) were found numerically by solving the linearized Navier-Stokes equation for incompressible flow (for details, see sections 1–5 in the Supporting Material), and thrombus shape was then adjusted according to a hydrodynamics-dependent growth rate.

Platelet accumulation

Platelets circulate in the blood, relatively inactive, and do not adhere to healthy vessel walls. Damage of a vessel wall starts a cascade of processes leading to formation of a thrombus (1). Its volume increases due to attachment of platelets supplied by the bloodstream. Platelet adhesion at the early stage is reversible (2,6), and thrombus growth rate is the balance of the rates of platelet attachment, j_{in}, and detachment, j_{out},

$$\frac{d}{dt}V_{thromb} = \int_{surf} (j_{in} - j_{out})dA, \qquad (1)$$

where the integral is taken over the thrombus surface capable of catching platelets. Platelet attachment indeed depends on hydrodynamic conditions (13,14,18,23–26). In our model, moving red blood cells (RBCs) influence platelet transport toward vessel walls based on the concept of shear-enhanced diffusivity (18,27–30), implicitly expressed as a shear-dependent platelet accumulation rate, j_{in}. We use a power-law function proposed earlier, $j_{in} \simeq \psi\dot{\gamma}^{1-\beta}$, with $\beta \approx 0.2$ for human blood cells. This expression comes from the supplementary materials in Tokarev et al. (18) and also from rigorous mathematical analysis by Tandon and Diamond (31). Platelet flux toward the wall is determined by the frequency of their near-wall inelastic collisions with erythrocytes (RBCs), as proposed in Tokarev et al. (18) and verified therein by comparison with experiments (27–29). Although collisions of platelets with platelets may be neglected (only collisions of platelets with RBCs are taken into account), j_{in} reads

$$j_{in} \approx \varepsilon(\dot{\gamma},\ d_{pl}/d_{RBC}) \times K d_{RBC} \Phi \dot{\gamma} c_{pl}, \qquad (2)$$

where c_{pl} is the platelet concentration in blood near the vessel wall, K is the coefficient dependent on shape and size of the platelets and RBCs, d_{RBC} and d_{pl} are the diameters of platelets and RBCs, respectively, Φ is the hematocrit, and $\dot{\gamma}$ is the shear rate at the vessel wall. The collision efficiency, $\varepsilon(\dot{\gamma},\ d_{pl}/d_{RBC})$, as a function of shear rate, has the power-law form (see Eq. S14 in the supplementary data of Tokarev et al. (18))

$$\varepsilon(\dot{\gamma},\ d_{pl}/d_{RBC}) = A \times \left(\frac{2.725}{\dot{\gamma}}\right)^{\beta}, \qquad (3)$$

where coefficient A and index β both depend only on the cell diameter ratio, d_{pl}/d_{RBC}. Thus, recasting this expression, we get the formula $j_{in} \simeq \psi\dot{\gamma}^{1-\beta}$, which we use in this article. Here, ψ is a parameter defined by the form and size of platelets and RBCs, the near-wall concentration of platelets in blood, and hematocrit. Index β depends on the sizes and mechanical properties of RBCs and platelets (18).

The thrombus erosion rate, j_{out}, should be proportional to viscous shear stress per unit area of thrombus, $\eta\dot{\gamma}$, where η is the viscosity of blood plasma, inversely proportional to interplatelet adhesive forces, and should depend on the shape and density of the platelet aggregate, $j_{out} = \xi_d\dot{\gamma}$, where ξ_d is a constant with a dimensionality of length, which accounts for all non-hydrodynamic effects. The effective growth rate, $k_{eff} = (j_{in} - j_{out})$, is a power function of the wall shear rate,

$$k_{eff} = \psi\dot{\gamma}^{1-\beta} - \xi_d\dot{\gamma}. \qquad (4)$$

This value is positive for small $\dot{\gamma}$, but changes its sign if $\dot{\gamma} > \dot{\gamma}_{cr}$, where $\dot{\gamma}_{cr} = (\psi/\xi_d)^{1/\beta}$ corresponds to a balance between the influx and outflux of platelets ($k_{eff} = 0$). Equation 4 is an approximate formula, but it reflects the experimentally observed behavior of platelet accumulation with respect to shear-rate change. The adhesion is absent without flow and increases initially with the increasing shear rate. However, for further increase of shear rate, the flow starts rupturing the thrombus (1,5,6), which leads to lowering of the platelet accumulation rate for high (>10^4 s^{-1}) shear rate (13,23,29).

In particular, for an axisymmetric thrombus ($\Theta = 2\pi$), the model permits analytical consideration. When the thrombus grows over the whole perimeter of the vessel cross section, the lumen has a circular shape with inner radius $r(t) < r_0$. Since the only variable that determines the size of an axisymmetric thrombus is the inner lumen radius, $r(t)$, in that case, Eq. 1 reads

$$-2\pi rl \times \frac{dr}{dt} = k_{\text{eff}}(\dot{\gamma}) \times A, \tag{5}$$

where $A \simeq 2\pi rl$ is the area capable of accumulating platelets, and $\dot{\gamma} = \Delta p_x(t) \times r(t)/(2\eta l)$ is the shear rate at the top surface of the thrombus (see section 4 in the Supporting Material).

For convenience, we introduce the following dimensionless values that determine thrombosis dynamics: the relative thrombus length, $\lambda = l/L$; the scaled vessel radius, $\rho_0 = r_0/L$; the inner radius of the lumen, $\rho = r/L$; the adhesion parameter, $\xi = (\dot{\gamma}_0/\dot{\gamma}_{\text{cr}})^{\beta} = \xi_d \times \dot{\gamma}_0^{\beta}/\psi$, which characterizes the stability of platelet aggregates subjected to hydrodynamic forces in a vessel; and $\Psi = \psi\dot{\gamma}_0^{1-\beta}\tau/L$, which determines the typical timescale, τ, for the dynamics of thrombosis. We define the typical scale for hydraulic resistance as

$$[R] = \frac{8\eta}{\pi L^3}. \tag{6}$$

As for the flow-rate scale, it is convenient to express this value through a combination of blood flow rate at the outlet of the heart, Q_0, and the shunting hydraulic resistance, R_w : $[Q] = Q_0R_w/[R]$. The pressure difference is thus scaled to a factor $[\Delta p] = Q_0R_w$. The shear rate in the stenosed vessel, $\dot{\gamma}$, was scaled to the initial shear rate (when no thrombus had yet grown):

$$\dot{\gamma}_0 = \frac{[\Delta p]\rho_0}{2\eta} = \frac{Q_0R_wr_0}{2\eta L}, \tag{7}$$

so that the dimensionless shear rate is $G = \dot{\gamma}/\dot{\gamma}_0$.

We note here the simplifying assumption of our model that thrombus growth is solely due to platelet aggregation. Our model does not consider explicitly the biochemistry of blood coagulation, which is indeed important (32) for clot formation. However, our approximation assumes that these effects are taken into account implicitly in the rate of platelet attachment estimated from the experimental data. What is important is the balance between the mechanical properties of the aggregate and the hydrodynamic forces acting to disrupt it. Besides that, recent reports (6) suggest that the general shape of thrombi and subocclusive thrombus stabilization are completely determined by the dynamics of the thrombus shell, which contains no fibrin/thrombin and is composed of platelets with only slight activation.

RESULTS

We performed numerical simulations to reveal the mechanism of thrombosis regulation. Fig. 2 suggests that a longer thrombus experiences lower shear stress on its surface. In Fig. 2, *a–c*, the maximal shear rate (and, thus, the force) on top of the plug gradually reduced fourfold when the length of the thrombus was increased from 50 μm to 500 μm. Our analytical calculations for the axisymmetric case ($\Theta_0 = 2\pi$) also support these findings, as illustrated in Fig. 2 *d*. Note the nonmonotonic dependence of shear rate on the degree of stenosis: when $\lambda \ll 1$, the shear rate increases with growing stenosis, reaches a maximum, $\dot{\gamma}_{\text{max}}$, and then goes to zero as occlusion occurs. That is consistent with earlier observations (15,33). Hydrodynamic shear forces, $f_{\text{h}} \propto \dot{\gamma}$, may prevent occlusion, if $\dot{\gamma}_{\text{max}}$ is high enough. Therefore, longer thrombi tend to be more occlusive. An increase in the relative shunting resistance lessens $\dot{\gamma}_{\text{max}}$ (Fig. 2 *e*), yet without changing the qualitative picture of

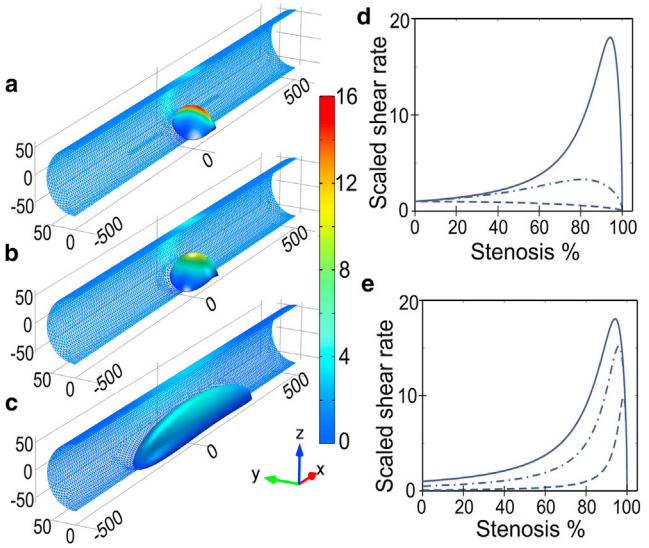

FIGURE 2 (*a–c*) Mapping of scaled shear rate, $\dot{\gamma}/\dot{\gamma}_0$, over the thrombus surface and walls of the blood vessel computed with finite-difference simulation for different lengths of a thrombus: 50 μm (*a*), 100 μm (*b*), and 500 μm (*c*). Vessel diameter is 100 μm. The pressure drop between the vessel's ends is $\Delta p_{12} = 100$ Pa. (*d*) Dependence of shear rate on degree of stenosis for $l/L = 0.01$ (*solid line*), 0.1 (*dash-dotted line*), and 0.75 (*dashed line*). Here, $R_w/[R] = 10^{-3}$ and $[R] = 8\eta/(\pi L^3)$. (*e*) Shear rate versus stenosis for different hydraulic resistances of the shunt: $R_w/[R] = 10^{-3}$ (*solid line*), 1 (*dash-dotted line*), and 10 (*dashed line*), and thrombus length is $l/L = 0.01$. To see this figure in color, go online.

thrombosis. For the realistic system, the limit $R_w \to 0$ (equivalent to $\Delta p_{12} = \text{const}$) is a good approximation (see section 5 in the Supporting Material). We note that Fig. 2 *e* shows the ratio of the actual dimensional shear rate at walls of a stenosed region to the initial wall shear rate (when the thrombus height is zero). For that reason, this plot resembles the relative changes due to stenosis with respect to the initial flow. Although smaller absolute values of shear rate in stenosed vessels are expected for smaller R_w, the relative change of shear rate due to growing stenosis is much more pronounced in that case. In other words, smaller R_w stands for higher sensitivity of the system to growing stenosis.

Good consistency with the experimental data attests to the validity of our theory (Fig. 3 *a*). We found model parameters ψ, ξ, and L by fitting experimental data from Sato and Ohshima (15) (for details, see section 8 and Fig. S5 in the Supporting Material). Specifically, we found that $\dot{\gamma}_{\text{cr}} \approx 3400\ \text{s}^{-1}$ corresponds to the balance between the influx and outflux of platelets in this particular experiment.

Thrombus growth rate, k_{eff}, can be positive or negative, depending on the system parameters, so that a thrombus can either grow or decrease in size. If we plot this value as a function of thrombus height (Fig. 3 *b*), the effective-growth-rate diagram characterizes the dynamics of thrombosis. We found that a saddle-node bifurcation takes place when the relative thrombus length, λ, is changing. If λ is above critical, the only stable point exists, corresponding

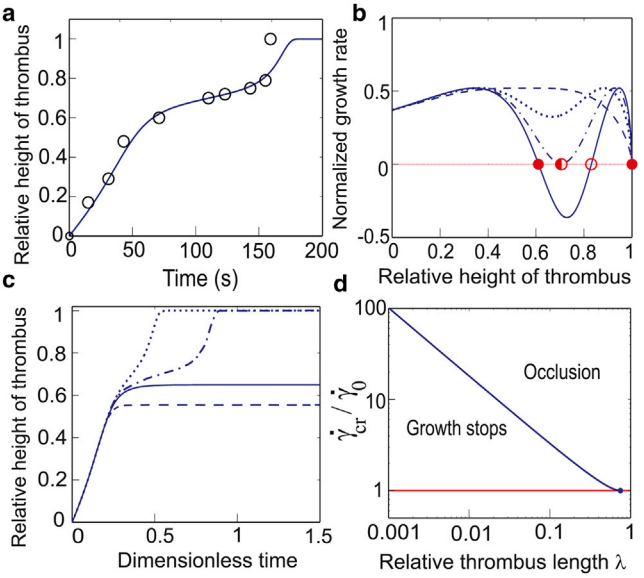

FIGURE 3 (*a*) Time course for changes in relative thrombus height in a venule with inner radius $r_0 = 31$ μm and length of injury $l = 4r_0$; $\dot{\gamma}_0 \approx 320$ s^{-1}. Theory (*solid line*) is compared to experiments from Sato and Ohshima (15) (*circles*); error bars are smaller than symbols. Dimensionless model parameters found from the fitting were $\Psi = 0.026$, $\xi = 0.63$, and $r_0/L = 5.8 \cdot 10^{-3}$. We also set $\beta = 0.2$ for all theoretical curves. (*b*) Phase portrait for the growth of an axisymmetric thrombus: the normalized effective thrombus growth rate, $k_{\text{eff}}/(\dot{\gamma}_0^{1-\beta}\psi)$, as a function of the ratio of thrombus height to vessel radius, h/r_0, for $\xi = 0.63$ and $r_0/L = 0.05$. Solid, dash-dotted, dotted, and dashed lines correspond to $\lambda = 0.016$, 0.022, 0.035, and 0.100, respectively. Solid and open circles mark stable and unstable equilibrium points, respectively, and the semisolid circle is the saddle node. (*c*) Growth dynamics of axisymmetric thrombi: for $\lambda = 0.028$ (*dotted line*) and 0.023 (*dash-dotted line*), occlusion occurs, whereas for 0.020 (*solid line*) and 0.005 (*dashed line*), the thrombus reaches a quiescent height and stops growing. Here, $\Psi = 0.05$, $\xi = 0.63$, and $r_0/L = 0.01$. Critical size of injury was found to be $\lambda_{\text{cr}} \simeq 0.022$. (*d*) Diagram of axisymmetric thrombosis. Normalized critical shear rate, $\dot{\gamma}_{\text{cr}}/\dot{\gamma}_0$, versus relative thrombus length, λ. To see this figure in color, go online.

to total occlusion. As λ decreases, a saddle-node fixed point emerges and then divides into two equilibrium points. The one with smaller h/r_0 is a locally stable node corresponding to a nonoccluding thrombus, and the other one is not stable.

Typical time courses for axisymmetric thrombi are presented in Fig. 3 *c* for different λ. The analysis shows that there exists a critical thrombus length, λ_{cr}, that differentiates the regimes of occlusion and thrombosis stoppage. For $\lambda > \lambda_{\text{cr}}$, the occlusion occurs in a finite period of time, and for $\lambda < \lambda_{\text{cr}}$, the thrombus reaches finite size. The value of λ_{cr} should be determined from the condition $\dot{\gamma}_{\max} = \dot{\gamma}_{\text{cr}}$, where $\dot{\gamma}_{\max}$ is the peak value of the dimensionless shear rate and $\dot{\gamma}_{\text{cr}}$ is the shear rate for which the average influx and outflux of platelets in Eq. 1 are balanced and $k_{\text{eff}} = 0$. This requirement leads to the equation (see section 9 in the Supporting Material for mathematical details)

$$\lambda^3(1-\lambda) = \frac{27}{256}\left(\frac{\dot{\gamma}_0}{\dot{\gamma}_{\text{cr}}}\right)^4. \qquad (8)$$

Note that $\dot{\gamma}_{\text{cr}}$ is a biological characteristic that depends on the adhesive properties of platelets, hematocrit, and sizes of cells, whereas $\dot{\gamma}_0$, the initial wall shear rate, is a hydrodynamical characteristic of the system that is only dependent on geometry and pressure. Solving Eq. 8 determines critical relative thrombus length, $\lambda_{\text{cr}} = l_{\text{cr}}/L$, so that if $\lambda > \lambda_{\text{cr}}$, the thrombosis always proceeds to occlusion, and for $\lambda < \lambda_{\text{cr}}$, the thrombus reaches a stable, nonocclusive size. A saddle-node bifurcation occurs at $\lambda = \lambda_{\text{cr}}$.

Fig. 3 *d* summarizes our findings for the axisymmetric thrombus in the form of a parametric diagram. The x axis of the diagram shows $\lambda = l/L$, and the y axis corresponds to $\dot{\gamma}_{\text{cr}}/\dot{\gamma}_0$. The upper-right corner of the diagram corresponds to parameters for which the thrombus grows to occlusion. The domain of thrombosis stoppage is enclosed between line $\lambda_{\text{cr}} = f(\dot{\gamma}_{\text{cr}}/\dot{\gamma}_0)$, found from Eq. 8, and the horizontal line $\dot{\gamma}_{\text{cr}} = \dot{\gamma}_0$. Below λ_{cr}, any platelet aggregate will be washed away by the bloodstream, as $\dot{\gamma}_0 > \dot{\gamma}_{\text{cr}}$.

Fig. 4 *a* suggests that nonsymmetric thrombi show more of a tendency to occlusion than ring-shaped thrombi. We found that thrombi with an initial angular size, Θ_0, close to 2π stopped their growth, since $\lambda < \lambda_{\text{cr}}$, yet injuries with smaller Θ_0 and the same λ led to occlusion. The threshold still remains for the nonsymmetric case, as shown in Fig. 4 *b*, but λ_{cr} becomes smaller for smaller Θ_0. According to our results, the highest possible shear rate is attained for the circular cross section (for mathematical details, see section 3 in the Supporting Material); thus, the ring-shaped thrombus leads to the most adverse conditions for occlusion.

The only dimensionless parameter defining the details of platelet adhesion is $\xi = (\dot{\gamma}_0/\dot{\gamma}_{\text{cr}})^{\beta}$. It quantifies the ratio of platelet detachment to accumulation rates. Fig. 5 *a* shows that higher ξ makes occlusion less plausible. The final size of the thrombus is determined by ξ (see Fig. 5 *b*). Suppression of platelet adhesion (increase of ξ) diminishes the size of a stable thrombus when $\lambda < \lambda_{\text{cr}}$. Note that occlusive equilibrium is stable for any λ.

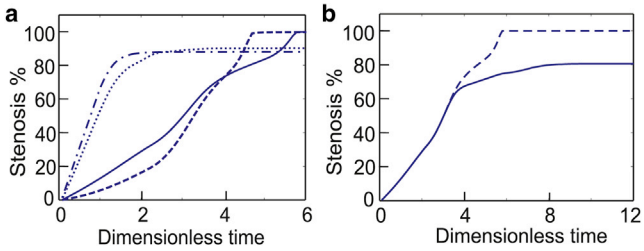

FIGURE 4 Dynamics of nonsymmetric thrombi. (*a*) Time courses for thrombi with initial angular sizes $\Theta_0 = \pi/3$ (*solid line*), $\pi/10$ (*dashed line*), $3\pi/2$ (*dash-dotted line*), and 2π (*dotted line*). Thrombus length is $\lambda = 0.018$ for all curves, a value that is smaller than λ_{cr} for the axisymmetric case. (*b*) Time courses for thrombi with $\Theta_0 = \pi/3$ and $\lambda = 0.018$ (*dashed line*), and 0.005 (*solid line*). $\Psi = 1.0$ and $\xi = 0.63$. To see this figure in color, go online.

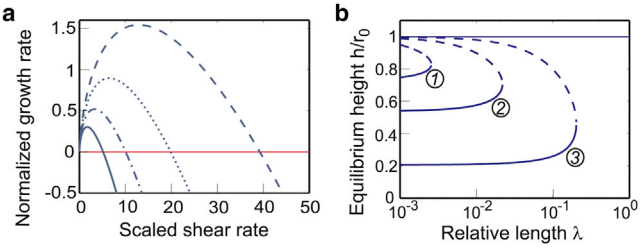

FIGURE 5 Effect of the adhesion strength parameter, ξ, on thrombosis. (*a*) Normalized effective growth rate, $k_{\text{eff}}/(\dot{\gamma}_0^{1-\beta}\psi)$, versus $\dot{\gamma}/\dot{\gamma}_0$: $\xi = 0.72$ (*solid line*), 0.63 (*dash-dotted line*), 0.55 (*dotted line*), and 0.48 (*dashed line*). (*b*) Bifurcation diagram for axisymmetric thrombus: solid and dashed lines show locally stable and unstable thrombus heights, respectively, in dependence on λ; $\xi \simeq 0.46$, 0.63, and 0.87 for curves *1–3*, respectively. To see this figure in color, go online.

DISCUSSION

Our results suggest that the mechanism of thrombus growth regulation in microvasculature rests on the interplay between the nontrivial hydrodynamics-dependent platelet-aggregation law (Eq. 4) and features of the microcirculatory network. Specifically, the initial prevalence of adhesion favors the formation of a hemostatic plug, yet the consequent increase of shear forces impedes thrombus growth and may eventually stop it. However, if injury length exceeds the critical value, this mechanism fails to prevent occlusion due to lesser shear rates. This explains why ferric-chloride-induced thrombosis characterized by vast injuries is usually occlusive (3,4), whereas small laser-induced thrombi may stop growing (6). Interestingly, recanalization of occlusive thrombi (34,35) and the risks of implant-induced thrombosis (36) also depend on the thrombus length in the same threshold manner.

The principal conclusion is the existence of a threshold injury length, $l_{\text{cr}} = \lambda_{\text{cr}} L$, demarcating regimes of thrombosis due to the occurrence of saddle-node bifurcation. This value depends on the relative adhesion strength, expressed via the fraction of $\dot{\gamma}_{\text{cr}} = (\psi/\xi_d)^{1/\beta}$ and initial wall shear rate, $\dot{\gamma}_0$ (Eq. 8). Another interesting thing is a noticeable bistability (Fig. 5 *b*) predicted for subcritical λ. The reasons for the observed dynamics are contained within the system itself. The positive feedback is provided by shear-dependent platelet margination, manifested in the aggregation rate, j_{in}, increasing with shear rate. The shear-rate peak effect (Fig. 2 *d*) serves as a mechanism to filter out small stimuli and acts together with thrombus erosion, $j_{\text{out}} \sim \dot{\gamma}$, to inhibit thrombosis (i.e., negative feedback) and prevent explosive growth. We note that such behavior comes naturally from the hydraulics of the system and is independent of the exact nature of platelet transport. What is essential is that j_{in} grows more slowly with shear rate than does j_{out}. Even without any collision-induced platelet margination, classical transport theories (27–29,37) imply that platelet transport to the wall will increase with shear rate as $\dot{\gamma}^{\alpha}$, with $\alpha<1$, so collision-induced margination is not principal for our results.

Remarkably, our conclusions complement the results of Beltrami and Jesty (38), who predicted mathematically that there exists a threshold size of a membrane patch for proteolysis and enzyme (thrombin) production during blood plasma coagulation. This fact discloses the fundamental generality of the described flow-dependent regulation mechanism. Apparently, in both systems the thresholds originate from the presence of feedback.

For a longer thrombus, depletion of platelets due to their attachment at the upstream region of the thrombus may become important. Thus, axial variations in its height are likely, which in turn affects the shear-rate distribution on the thrombus and, potentially, its further growth. However, if this is the case, the hydrodynamic (shear) forces at the thrombus surface would be greater in the upstream region with higher stenosis, decreasing local growth rate k_{eff}, and so leveling the height of a plug. In vivo experiments (see supplementary information in Stalker et al. (6)) support this idea: loosely packed upper layers of a thrombus are facilely smeared by the flow. In any case, the occlusion event would be governed by the region of highest stenosis, for which our model should give qualitatively correct results.

Our analysis is restricted to platelet thrombi in venules and arterioles and does not consider larger blood vessels. In the latter case, one should correct the hydrodynamic values to account for nonlaminar flows (19). Furthermore, as we focus on the effects caused by hydrodynamics, the difference between arterioles and venules from this point is rather quantitative (19), and no specific modification of our model is required to switch between these types of vessels. The theory presented here does not describe the stage of initiation of thrombus growth and the lag time, as this is not the aim of our research. We also do not consider explicitly a number of biological processes and features (platelet activation, fibrin growth, granule secretion, extent of damage, tissue-factor concentration, etc.) that take place inside the core (6) of the thrombus and basically cannot alter the surface-related hydrodynamic mechanism considered here. These processes, naturally addressed to strengthen the plug (2), would correct quantitative estimations of thrombus growth dynamics but would not principally change the hydrodynamic effects, which are central to our study.

Our model is inspired by experimental observations about thrombus structure, in particular by Stalker et al. (6), which clearly show that platelets attach to and detach from a relatively thin interfacial layer, called a shell, in contrast to the core, which consists of firmly attached platelets partly covered with fibrin. Within the shell, which has a thickness of several platelets, whole parts of a clot (whole platelet aggregates) can detach, not only the individual cells. Note that our formulation includes this fact, since the detachment rate is described in our model by parameter ξ_d, which can be varied in a wide range.

Finally, length of the plug may change during thrombosis (1,6). However, this elongation is usually moderate (smaller than an order of magnitude) and is not radical for microvascular thrombi, based on experimental evidence (39) that the adhesive substrate/activator area limits the length of the resulting thrombus for small concentrations of tissue factor at the injury site. It was shown experimentally that an assumption of constant thrombus length is quite adequate, as long as activation is not very strong (tissue factor concentration is moderate; compare to results presented in Okorie et al. (40)). Therefore, our analysis is precise if injury is not very severe and concentration of activators near the injury site is moderate. We believe that for a strong activation, the exact value of critical length, λ_{cr}, could change, but our qualitative results would not be principally affected. In addition, since the dependence of vascular resistance R_x of the thrombotic region is dependent on length l much more weakly than on lumen radius r (powers of 1 and 4, respectively; see section 4 of the Supporting Material), one may expect that the main effect on the blood flow (and thus on platelet accumulation rate) would be from changes of lumen radius r, whereas alterations of l are secondary in the considered system. This can be seen in Fig. 2 *d*: to switch from the solid line to the dash-dotted line, we have to change $\lambda = l/L$ through the whole order of magnitude (from 0.01 (*solid line*) to 0.1 (*dash-dotted line*)). However, qualitatively, the curve for shear rate has the same hillock shape. For $\lambda<0.01$, the change in these curves is even smaller: we cannot distinguish between lines for 0.005 and 0.01 in this figure. Since shear-rate increase is the principal regulator of the occlusion event, our assumption of constant thrombus length is expected to give reasonably precise results when the injury is sufficiently small ($\lambda \leq 0.01$).

Several effects predicted by our theory are not obvious. The most direct approach to experimental verification is to study thrombus formation under constant pressure conditions using different sizes of the damaged area. We stress that shunt-vessel R_w must be implemented in the experimental setup to correctly reproduce microvascular hemodynamics and thrombosis in vitro. Our model predicts that there should be a triggering from occlusion to a stable thrombus for a certain length of injury. Another way is to lower $\dot{\gamma}_{cr}/\dot{\gamma}_0$ by using platelets with partial adhesion receptor deficiencies, or to increase pressure, Δp_{12}.

CONCLUSION

In this work, using only basic physical principles, not involving complex biochemical concepts, we quantitatively describe the switching mechanism in microvascular thrombosis. Our findings resolve fundamental contradictions in experiments and constitute an essential step toward understanding and treatment of different thrombotic disorders. Our results are widely applicable outside the hemostasis field. For example, blood-clotting-inspired colloid-polymer composite systems (41) are an attractive class of new smart materials with tunable properties. The dynamics of growth of these artificial plugs depends mostly on the shear rate and the strength of the polymer-colloid binding potential, and no biochemical activation is required. We believe that our theory describes such artificial clotting systems as well, providing a basis for their usage in numerous applications, e.g., microfluidic devices.

SUPPORTING MATERIAL

Supporting Materials and Methods and six figures are available at http://www.biophysj.org/biophysj/supplemental/S0006-3495(15)00601-3.

AUTHOR CONTRIBUTIONS

A.V.B. developed a model, carried out the calculations, and analyzed results; M.A.P. analyzed the results; and F.I.A. outlined the scientific problem and analyzed the results. All authors reviewed the manuscript.

ACKNOWLEDGMENTS

This study was supported by the Russian Science Foundation (grant number 14-14-00195) with the exceptions of computational fluid dynamics simulations of blood flow in a thrombotic vessel and calculations of growth dynamics for nonaxisymmetric thrombus, which were supported by the Stipend of the President of Russian Federation for young scientists (grant number SP-2427.2015.4).

REFERENCES

1. Furie, B., and B. C. Furie. 2005. Thrombus formation in vivo. *J. Clin. Invest.* 115:3355–3362.
2. Jackson, S. P., W. S. Nesbitt, and E. Westein. 2009. Dynamics of platelet thrombus formation. *J. Thromb. Haemost.* 7 (*Suppl 1*):17–20.
3. Kurz, K. D., B. W. Main, and G. E. Sandusky. 1990. Rat model of arterial thrombosis induced by ferric chloride. *Thromb. Res.* 60:269–280.
4. Denis, C. V., and D. D. Wagner. 2007. Platelet adhesion receptors and their ligands in mouse models of thrombosis. *Arterioscler. Thromb. Vasc. Biol.* 27:728–739.
5. Falati, S., P. Gross, …, B. Furie. 2002. Real-time in vivo imaging of platelets, tissue factor and fibrin during arterial thrombus formation in the mouse. *Nat. Med.* 8:1175–1181.
6. Stalker, T. J., E. A. Traxler, …, L. F. Brass. 2013. Hierarchical organization in the hemostatic response and its relationship to the platelet-signaling network. *Blood.* 121:1875–1885.
7. Kuijpers, M. J. E., K. Gilio, …, J. W. Heemskerk. 2009. Complementary roles of platelets and coagulation in thrombus formation on plaques acutely ruptured by targeted ultrasound treatment: a novel intravital model. *J. Thromb. Haemost.* 7:152–161.
8. Oude Egbrink, M. G., G. J. Tangelder, …, R. S. Reneman. 1991. Fluid dynamics and the thromboembolic reaction in mesenteric arterioles and venules. *Am. J. Physiol.* 260:H1826–H1833.
9. Fogelson, A. L., and R. D. Guy. 2004. Platelet-wall interactions in continuum models of platelet thrombosis: formulation and numerical solution. *Math. Med. Biol.* 21:293–334.
10. Skorczewski, T., L. C. Erickson, and A. L. Fogelson. 2013. Platelet motion near a vessel wall or thrombus surface in two-dimensional whole blood simulations. *Biophys. J.* 104:1764–1772.

11. Maxwell, M. J., E. Westein, …, S. P. Jackson. 2007. Identification of a 2-stage platelet aggregation process mediating shear-dependent thrombus formation. *Blood.* 109:566–576.
12. Tosenberger, A., F. Ataullakhanov, …, V. Volpert. 2013. Modelling of thrombus growth in flow with a DPD-PDE method. *J. Theor. Biol.* 337:30–41.
13. Begent, N., and G. V. R. Born. 1970. Growth rate in vivo of platelet thrombi, produced by iontophoresis of ADP, as a function of mean blood flow velocity. *Nature.* 227:926–930.
14. Richardson, P. D. 1973. Letter: Effect of blood flow velocity on growth rate of platelet thrombi. *Nature.* 245:103–104.
15. Sato, M., and N. Ohshima. 1986. Hemodynamics at stenoses formed by growing platelet thrombi in mesenteric microvasculature of rat. *Microvasc. Res.* 31:66–76.
16. Pivkin, I. V., P. D. Richardson, and G. Karniadakis. 2006. Blood flow velocity effects and role of activation delay time on growth and form of platelet thrombi. *Proc. Natl. Acad. Sci. USA.* 103:17164–17169.
17. Xu, Z., N. Chen, …, M. Alber. 2009. Study of blood flow impact on growth of thrombi using a multiscale model. *Soft Matter.* 5:769–779.
18. Tokarev, A. A., A. A. Butylin, and F. I. Ataullakhanov. 2011. Platelet adhesion from shear blood flow is controlled by near-wall rebounding collisions with erythrocytes. *Biophys. J.* 100:799–808.
19. Fung, Y. C. 1997. Biomechanics: circulation, 2nd ed. Springer-Verlag, New York.
20. Caro, C. G., T. J. Pedley, …, W. A. Seed. 1978. The Mechanics of Che circulation. Oxford University Press, Oxford, United, Kingdom.
21. Fuster, V., R. W. Alexander, …, I. Nash. 2004. Hurst's The Heart, 11th ed. McGraw-Hill, New York.
22. Fung, Y. C. 1993. Biomechanics: Mechanical Properties of Living Tissues, 2nd ed. Springer, New York.
23. Turitto, V. T., H. J. Weiss, and H. R. Baumgartner. 1980. The effect of shear rate on platelet interaction with subendothelium exposed to citrated human blood. *Microvasc. Res.* 19:352–365.
24. Baumgartner, H. R. 1973. The role of blood flow in platelet adhesion, fibrin deposition, and formation of mural thrombi. *Microvasc. Res.* 5:167–179.
25. Sato, M., and N. Ohshima. 1990. Effect of wall shear rate on thrombogenesis in microvessels of the rat mesentery. *Circ. Res.* 66:941–949.
26. Zhao, H., and E. S. G. Shaqfeh. 2011. Shear-induced platelet margination in a microchannel. *Phys. Rev. E Stat. Nonlin. Soft Matter Phys.* 83:061924.
27. Turitto, V. T., and H. R. Baumgartner. 1975. Platelet deposition on subendothelium exposed to flowing blood: mathematical analysis of physical parameters. *Trans. Am. Soc. Artif. Intern. Organs.* 21:593–601.
28. Turitto, V. T., and H. R. Baumgartner. 1975. Platelet interaction with subendothelium in a perfusion system: physical role of red blood cells. *Microvasc. Res.* 9:335–344.
29. Turitto, V. T., and H. R. Baumgartner. 1979. Platelet interaction with subendothelium in flowing rabbit blood: effect of blood shear rate. *Microvasc. Res.* 17:38–54.
30. Bark, Jr., D. L., and D. N. Ku. 2013. Platelet transport rates and binding kinetics at high shear over a thrombus. *Biophys. J.* 105:502–511.
31. Tandon, P., and S. L. Diamond. 1997. Hydrodynamic effects and receptor interactions of platelets and their aggregates in linear shear flow. *Biophys. J.* 73:2819–2835.
32. Anand, M., K. Rajagopal, and K. R. Rajagopal. 2006. A viscoelastic fluid model for describing the mechanics of a coarse ligated plasma clot. *Theor. Comput. Fluid Dyn.* 20:239–250.
33. Colace, T. V., R. W. Muthard, and S. L. Diamond. 2012. Thrombus growth and embolism on tissue factor-bearing collagen surfaces under flow: role of thrombin with and without fibrin. *Arterioscler. Thromb. Vasc. Biol.* 32:1466–1476.
34. Riedel, C. H., P. Zimmermann, …, O. Jansen. 2011. The importance of size: successful recanalization by intravenous thrombolysis in acute anterior stroke depends on thrombus length. *Stroke.* 42:1775–1777.
35. Strbian, D., T. Sairanen, …, P. J. Lindsberg. 2014. Intravenous thrombolysis of basilar artery occlusion: thrombus length versus recanalization success. *Stroke.* 45:1733–1738.
36. Suh, J., D.-W. Park, …, S.-J. Park. 2010. The relationship and threshold of stent length with regard to risk of stent thrombosis after drug-eluting stent implantation. *JACC Cardiovasc. Interv.* 3:383–389.
37. Zydney, A. L., and C. K. Colton. 1988. Augmented solute transport in the shear flow of a concentrated suspension. *PhysicoChem. Hydrodyn.* 10:77–96.
38. Beltrami, E., and J. Jesty. 2001. The role of membrane patch size and flow in regulating a proteolytic feedback threshold on a membrane: possible application in blood coagulation. *Math. Biosci.* 172:1–13.
39. Colace, T. V., J. Jobson, and S. L. Diamond. 2011. Relipidated tissue factor linked to collagen surfaces potentiates platelet adhesion and fibrin formation in a microfluidic model of vessel injury. *Bioconjug. Chem.* 22:2104–2109.
40. Okorie, U. M., W. S. Denney, …, S. L. Diamond. 2008. Determination of surface tissue factor thresholds that trigger coagulation at venous and arterial shear rates: amplification of 100 fM circulating tissue factor requires flow. *Blood.* 111:3507–3513.
41. Chen, H., M. A. Fallah, …, A. Alexander-Katz. 2013. Blood-clotting-inspired reversible polymer-colloid composite assembly in flow. *Nat. Commun.* 4:1333.